Study of heat transfer and kinetics parameters influencing the design of heat exchangers for hydrogen storage in high-pressure metal hydrides

Milan Visaria [a], Issam Mudawar [a,*], Timothée Pourpoint [b], Sudarshan Kumar [c]

[a] School of Mechanical Engineering, Purdue University, West Lafayette, IN 47907, United States
[b] School of Aeronautics and Astronautics Engineering, Purdue University, West Lafayette, IN 47907, United States
[c] General Motors Research and Development Center, Warren, MI 48085, United States

ABSTRACT

This paper discusses the challenges of using hydrogen fuel cells to power light-duty vehicles. Storing sufficient amounts of hydrogen to cover adequate travel distances before refueling is one of the more pressing challenges, and different materials have been recommended to enhance storage capacity. This study concerns one class of storage materials called high-pressure metal hydrides (HPMHs). The most important component of a hydrogen storage system utilizing HPMHs is the heat exchanger, which, aside from storing the HPMH, must providing sufficient cooling during the hydrogen refueling to achieve the required short fill time of less than 5 min. Discussed in this paper are practical heat exchanger design guidelines for storage systems employing materials with high rates of heat generation during refueling. Most important among those is the maximum distance between the HPMH powder and the cooling surface, which, for $Ti_{1.1}CrMn$, must be kept below 10 mm to achieve a fill time of 5 min. A new parameter called non-dimensional conductance (NDC) is developed, which serves as a characteristic parameter to estimate the effects of various parameters on the reaction rate. Overall, it is shown that the hydrogen fill time is sensitive mostly to the effective thermal conductivity of the HPMH and the coolant's temperature, followed by the contact resistance between the powder and cooling surface.

© 2009 Elsevier Ltd. All rights reserved.

1. Introduction

1.1. Hydrogen potential and challenges

Energy demand across the globe has risen sharply over the last decade. Today, fossil-fuel-based sources of energy are being depleted at a fast rate because of the ever-increasing energy consumption. Additionally, fossil-fuels are contributing to both greenhouse gas emissions and global warming. The growing energy demands, along with the increasing environmental awareness, have created an urgent need for abundant and cleaner alternatives to fossil-fuels. Great advances have been made in converting freely available solar energy, wind energy, etc., into different useable energy forms. With current state of the art, these technologies are expensive and efforts are being made to make them both energy-efficient and cost-effective.

Among various sustainable energy solutions being explored, researchers believe hydrogen is a promising and suitable one. Aside from being the most abundant element on Earth, hydrogen is lightweight, can be produced via numerous technologies, and

produces water as a result of oxidation. This means that careful and intelligent use of hydrogen can ensure a virtually unlimited and environmentally safe source of energy. It also has high energy content per unit mass and hence is an obvious contender for an efficient energy source/carrier. These attributes explain the recent attention being placed on all aspects of hydrogen, from production to storage to use.

There are several important challenges to overcome before hydrogen can become a viable fuel. Only 1% of the hydrogen is available as molecular hydrogen gas while the majority is present in the form of water or hydrocarbons. Large-scale production of hydrogen from water or other chemical compounds in an efficient and clean method remains a challenge. Another challenge is storage volume. Though hydrogen has high energy content by weight (three times that of gasoline), its energy content by volume is only one-tenth that of gasoline. This poses major storage volume problems in automotive and other mobile systems with stringent volume constraints. A third challenge is hydrogen transport to filling stations. Because of the low density of hydrogen, finding an economical way of transporting large amounts of hydrogen to various locations is quite illusive. The fourth challenge is the use of hydrogen as a fuel in producing clean energy that would justify its wide acceptance in the market. Hydrogen can be used to produce energy

Nomenclature

C_a	hydriding constant or activation rate (s^{-1})		t	time (s)
c_p	specific heat (J/kg K)		T	temperature (K)
E_a	activation energy (J/mol-H_2)		$wt\%$	hydrogen storage capacity or hydrogen to metal hydride
F	fraction of reaction progress or progress variable			mass ratio when completely hydrided
ΔH_r	enthalpy of formation (J/mol-H_2)		x	distance coordinate (mm)
h	convective heat transfer coefficient (W/m^2 K)			
k	thermal conductivity (W/m K)		*Greek symbols*	
L	metal hydride thickness (mm)		ϕ	porosity
MW	molecular weight		ρ	density
NDC	non-dimensional conductance			
P	pressure (N/m^2)		*Subscripts*	
P_{eq}	equilibrium pressure (N/m^2)		Al	aluminum
P_o	ambient pressure (N/m^2)		des	desired
$\dot{q}'''$	volumetric heat generation rate (W/m^3)		f	coolant
R	universal gas constant (J/mol K)		H_2	hydrogen
R_{tc}	contact resistance (mm^2 K/W)		MH	high-pressure metal hydride
ΔS	entropy of reaction (J/mol-H_2 K)			

either by burning with oxygen in air (*e.g.*, internal combustion engine), or by electrochemical reaction with oxygen using fuel cells. Fuel cells are both energy efficient and virtually pollution free compared to internal combustion engines. The choice of energy production method is dictated mainly by cost and application. In summary, the advantages of using hydrogen as fuel can be realized only if all the relevant processes, from production to storage to energy generation, are clean and efficient.

1.2. Storage concerns for automobiles

The present work concerns the design of on-board hydrogen storage systems for automobiles. In mobile applications like automobiles, size and weight are crucial design factors. Apart from storing the required amount of hydrogen in a vehicle, it is essential to fill it in an acceptable period of time. Using a fuel cell stack, a vehicle can travel at least 300 miles using about 5 kg of hydrogen before it needs to be refueled [1]. The revised U.S. Department of Energy (DOE) targets for the year 2010 are 4.2 min to refill 5 kg of hydrogen, and a gravimetric capacity of 0.045 kg H_2/kg system (or 4.5 wt%) and a volumetric capacity of 28 g H_2/L system [2]. A commercial large-scale production-ready on-board hydrogen storage system must satisfy these size, weight and fill-time criteria, although slight variation are being adopted due to technological limitations. The storage system must also be safe, cost-effective and meet the fuel cell hydrogen demands under any environmental conditions. It is also desirable that the hydrogen storage technology be introduced with minimum alterations to the already present infrastructure.

1.3. Hydrogen storage options

Hydrogen can be stored either in gaseous form, liquid form or in the form of reversible compounds with certain metals or alloys. Due to the very low density of hydrogen gas, it has to be compressed to very high pressures (350–700 bar) to store sufficient quantities for vehicular use [3–4]. The primary advantages of compressed gas storage are simplicity and fast filling. However, compressed gas storage has low volumetric and gravimetric density (25 g/L and 4.6 wt%, respectively, at 700 bar [3–5]) compared to other storage options. Also, large amounts of energy are consumed in compressing hydrogen to such high pressures.

Liquid hydrogen can be stored at atmospheric pressure in cryogenic tanks at very low temperatures (~20 K). Liquid hydrogen has

relatively high volumetric capacity, is easy to transport, and can be filled in a short time, but large amounts of energy are required for the liquefaction process [3–4]. Also, at such low temperatures, it is virtually impossible to prevent boil-off. Hence, liquid hydrogen requires a cryostat with a highly efficient thermal management system for both the storage and the delivery vessels. This greatly compromises the high volumetric capacity of liquid hydrogen. Due to the size and weight of the insulated storage tanks and accessories, it is advantageous to store liquid hydrogen in relatively large quantities, which is why this form of storage is preferred for long haul, heavy-duty vehicles. A recent noteworthy development in liquid hydrogen storage is the Lawrence Livermore National Laboratory cryogenic insulated pressure vessel, which is capable of storing 10.7 kg H_2. This system uses an aluminum-lined composite-wrapped (Type 3) vessel with storage capacities of 7.4 wt% and 45.2 g/L [6–7].

Apart from storing hydrogen in gaseous and liquid form, it can also be stored in solid state in the form of chemical compounds. One of the forms of solid-state hydrogen storage is chemical hydrides. They are compounds that release hydrogen upon reacting with water or thermal decomposition (*e.g.*, NH_3BH_3, $C_{10}H_{18}$, $NaBH_4$). Chemical hydrides have the highest material volumetric capacities compared to all other forms of hydrogen storage. They also have the highest gravimetric capacities amongst all solid-state hydrogen storage methods [3–4,8] and eliminate the need to transport hydrogen from refinery to filling station. However, regeneration of these hydrides is problematic because the dehydriding reaction is not easily reversible. Once dehydrided, chemical hydrides have to undergo off-board processing before they can be reused. Some of the chemical hydrides may require large quantities of water to release the hydrogen, which presents storage system volume issues. Those challenges are major barriers to the widespread acceptance of this form of hydrogen storage.

Metal hydrides are metal compounds or alloys that react reversibly with hydrogen to form hydrides. Metal hydrides useful for on-board hydrogen storage can broadly be classified into complex metal hydrides and high-pressure metal hydrides (HPMH). Complex metal hydrides (*e.g.*, $NaAlH_4$, $LiBH_4$) have low hydriding pressures, in the range of 20–150 bar, but relatively high hydriding temperatures (200–300 °C) as well as high enthalpy of reaction [4]. They cover a wide range of hydriding pressures, temperatures and material capacities and typically possess high volumetric capacity. Their high desorption temperatures are undesirable because of the need to heat up the hydride to release hydrogen, thus lowering overall

system efficiency. In general, the hydriding and dehydriding processes in complex metal hydrides are very sensitive to temperature. If the temperature is close to equilibrium during the exothermic hydriding reaction, the filling rate can be very slow. Thus, complex metal hydride systems require external cooling, which substantially increases system weight and volume.

High-pressure metal hydrides (HPMHs) have high hydriding pressures and can be stored at up to 700 bar but moderate temperatures of less than 100 °C [9]. Widely studied HPMHs are Ti–Cr–Mn-based transition metal alloys. The gravimetric capacities of these materials (2–3 wt%) are smaller than any other storage materials and, like complex metal hydrides, these also require active cooling during hydriding to achieve faster fill rates; the hydrogen release can be controlled by varying the pressure and/or temperature. Due to the high pressures employed in these systems and high alloy densities, HPMH systems have amongst the highest volumetric capacities ($\sim$40 g/L) of all storage systems. However, they suffer low gravimetric capacity, mainly due to poor hydrogen absorption capacities and additional system weight of both the high-pressure cylinders and cooling hardware.

Recently, carbon-based physisorbing materials like CNTs and MOFs have shown great potential as hydrogen storage materials. Unlike metal hydrides, which store hydrogen by chemisorption, carbon-based physisorbing materials hold hydrogen on the surface via weak Van der Waal's forces. Material storage capacities of 6–7 wt% H_2 have been measured at 77 K and 50–100 bar [4,10]. These

Fig. 1. Capacity comparison of different storage techniques (adapted from [8,11]).

materials have low volumetric capacities and their hydrogen adsorption capacity greatly decreases with increasing temperature.

Thus, at present, no hydrogen storage technology satisfies all requirements of on-board storage for mobile applications. Fig. 1 shows volumetric and gravimetric capacities of various storage materials and compares them to the best-known system capacities using these materials. Without taking into account system cost or energy spent on storage, liquid hydrogen is the only storage option that meets the revised DOE targets for the year 2015. All other storage options fall short of the 2010 and 2015 targets, let alone the ultimate targets. To achieve these targets, it is important to develop new materials with better kinetic and thermal properties as well as storage systems with greater volumetric and gravimetric efficiencies. The different hydrogen storage options are compared in Table 1 based on their properties and performance parameters.

1.4. Challenges with high-pressure metal hydride storage and objectives of study

At the Purdue University Hydrogen Systems Laboratory (HSL), efforts are focused on both material characterizations and large-scale system development using HPMHs and carbon-based cryosorbents as storage materials. The present study concerns the design of hydrogen storage vessels using the HPMH $Ti_{1.1}CrMn$.

Despite its high volumetric capacity ($\sim$50 g/L), $Ti_{1.1}CrMn$ poses several challenges when implemented in hydrogen storage. First, its gravimetric capacity is relatively low, less than 2 wt% H_2 [14], which, along with high density of the base alloy, increase the weight of the storage system. A second challenge is low thermal conductivity. When activated (repeated cycles of cooling at high pressure and heating under vacuum), metal hydride powder has a particle size range of 5–20 μm, but the powder has a tendency to break into finer particles after repeated hydriding and dehydriding cycles. During the hydriding reaction, hydrogen atoms occupy the interstitial sites within the metal hydride matrix cells causing metal hydride expansion. As a result, the effective thermal conductivity of metal hydrides is quite low, about 1 W/m K [15]. A third challenge is tackling both the large amount of heat released during the hydriding reaction and the heat input during the dehydriding reaction. The hydriding reaction is kinetically driven and its rate depends on the temperature of the metal hydride. In order for the hydriding reaction to proceed at the desired rate, it is very important that the released heat be removed efficiently and, for a given pressure, the system temperature maintained below the
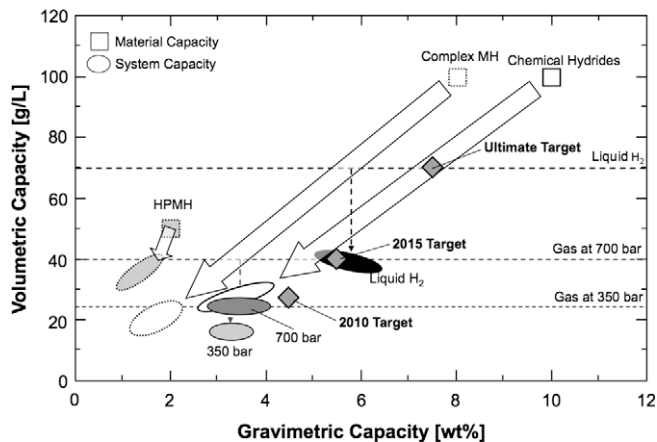
Table 1
Comparison of hydrogen storage technologies.

	Compressed H_2 gas [3–5]	Liquid H_2 [3,4,6,7]	Chemical hydride [3–4,8]	Complex MH [4,11–13]	HPMH [19]	Physisorbing materials [4,10]
Storage/charging pressure	Up to 700 bar	1–2 bar	1–2 bar	$\sim$150 bar	Up to 500 bar	20–40 bar
Storage temperature	Room temp.	20 K	Room temp.	$\sim$500 K	$\sim$350 K	$\sim$77 K
Material and system volumetric capacity (g/L)	40 Sys (25)	70.8 Sys (30–35)	100 Sys (30)	100 (30–160) Sys (20–30)	50–150 Sys (40)	30–40
Material and system gravimetric capacity (wt%)	Sys (4.7 at 700 bar)	Sys (5–6)	10 Sys (3–4)	4–7 Sys (1–2)	2–3 Sys (1–2)	4–8 Sys (2–4)
Fill time (min)	5–10	7–9	N/A	8–12 min	5 min	10 min
Onboard reversible	Yes	Yes	No	Yes	Yes	Yes
Desorption temperature, pressure	Room temp., 3.5 bar	N/A	>500 K, 3.5 bar	400 K, 3.5 bar	Room temp., 3.5 bar	77–100 K, 3.5 bar
Durability and repeatability	N/A	N/A	Need to be regenerated for reuse	Sensitive to impurities	Sensitive to impurities	Sensitive to impurities
Reactivity to air and moisture	N/A	N/A	Stable, no	Pyrophoric materials, Yes.	Pyrophoric materials.	Yes
Heat of reaction	N/A	N/A	$\sim$55 kJ/mole H2	$\sim$40 kJ/mole H2	$\sim$15–25 kJ/mole	$\sim$4–6 kJ/mole

equilibrium temperature of the hydride. This is why the most important component of a hydrogen storage system using HPMHs is the heat exchanger, evidenced by several recent efforts to develop heat exchangers for hydrogen storage using both complex metal hydrides [12–13,16,17–19] and HPMHs [9]. Poor thermal properties of metal hydride powder render the design of an efficient HPMH heat exchanger quite challenging. This task is complicated by the stringent space constraints of automotive systems. With this limited space, it is desired to maximize the volume of the HPMH, which means the heat exchanger must occupy the least volume possible.

The primary objective of this study is to understand the influences of various kinetic and thermal parameters on heat exchanger design, and to develop a scalable approach to designing a heat exchanger that is both compact and can achieve the goal of filling hydrogen gas within 5 min.

2. Model description

2.1. Model setup

The heat released by the hydriding reaction is absorbed by a liquid coolant. The HPMH heat exchanger is therefore a thermal device that dissipates heat from a metal hydride powder to the liquid coolant across the metallic wall of the coolant passage as illustrated in Fig. 2(a). Obviously, coolant passages must be configured to maintain close proximity to the powder in order to effectively dissipate the released heat of reaction. On the other hand, the volume occupied by the coolant passages must be minimized to maximize the volume available for the hydride powder. This goal is achieved by maximizing the thickness of hydride powder away from the coolant passage while both completing the hydriding reaction within 5 min and dissipating the released heat. The maximum hydride powder thickness is a key design parameter for any HPMH heat exchanger.

Fig. 2(b) shows the schematic for the model that is used to estimate the maximum hydride powder thickness. Using thermal symmetry between adjacent coolant passages, the metal hydride powder has a variable thickness L, half the thickness of powder between coolant passages, and is insulated along the plane of symmetry. The coolant is at temperature T_f and supplied at a flow

rate that yields a convective coefficient of h_f. The coolant passage is made of aluminum and has a thickness L_{Al}. Since the metal hydride powder and aluminum surface will not be in perfect contact, a contact resistance is assumed between the two.

2.2. Governing equations

One-dimensional transient conduction with internal heat generation in the metal hydride powder is given by

$$k_{MH} \frac{\partial^2 T}{\partial x^2} + \dot{q}''' = \rho_{MH} c_{p,MH} \frac{\partial T}{\partial t}, \tag{1}$$

where k_{MH}, ρ_{MH} and $c_{p,MH}$ are the effective thermal conductivity, density and specific heat of the powder, respectively, and $\dot{q}'''$ the rate of volumetric heat generation. It is assumed that the powder initially has uniform temperature and is completely dehydrided. Metal hydride properties are assumed to be uniform and constant throughout the simulation. Heat generation rate is the sum of heat of reaction and heat of pressurization (accounts for less than 10% of the total heat generated).

$$\dot{q}''' = \frac{dF}{dt} \frac{(wt\%)\rho_{MH}}{MW_{H_2}} \Delta H_r + \phi \frac{dP}{dt}, \tag{2}$$

where F, MW_{H_2}, ΔH_r, ϕ and P are the fraction of reaction progress (or progress variable), molecular weight of hydrogen, enthalpy of formation, porosity and pressure, respectively. Heat of reaction depends on the rate at which hydrogen is absorbed and increases with increasing hydriding (fill) rate. The reaction rate used in this study is based on an expression for hydrogen absorption in LaNi$_5$ derived by Mayer et al. [20–21] that assumes 1st order kinetics (which is typically observed in metal hydrides).

$$\frac{dF}{dt} = C_a \exp\left(\frac{-E_a}{RT}\right) \ln\left(\frac{P}{P_{eq}}\right)(1 - F), \tag{3}$$

where C_a, E_a, R and P_{eq} are the hydriding constant (or activation rate), activation energy, universal gas constant and equilibrium pressure, respectively. The equilibrium pressure in Eq. (3) is given by van't Hoff equation

$$P_{eq} = P_o \exp\left(\frac{\Delta H_r}{RT} - \frac{\Delta S}{R}\right), \tag{4}$$
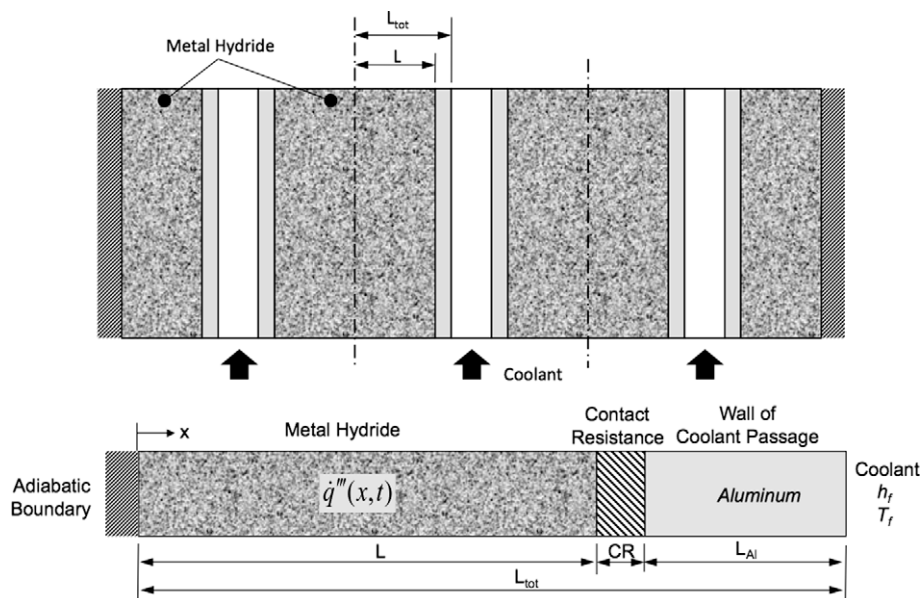
Fig. 2. Definition of metal hydride thickness in heat exchanger, and model used to determine maximum metal hydride thickness.

where P_o and ΔS are the ambient pressure and entropy of reaction, respectively. The above coupled heat diffusion and temperature-dependent kinetic equations are solved numerically over the metal hydride domain using the finite volume technique for different values of various parameters to understand the influence of these parameters on hydriding rate.

2.3. HPMH properties

High-pressure metal hydrides need to be activated before they can absorb hydrogen. Non-activated or oxidized metal hydrides have a particle size that is typically too large ($\sim$100 μm) to enable hydrogen absorption. They need to undergo an activation process, which consists of repeated cycles of cooling under high-pressure and heating under vacuum. This causes the hydride to break into particles that are small enough (less than 10 μm) to react with hydrogen. Once activated, the metal hydride spontaneously ignites upon exposure to air or any oxidizer. Since the hydride is composed of transition metal, the ignition temperature is as high as 1000 °C. This pyrophoric nature of activated metal hydride and the high-pressures involved make property measurements of HPMHs extremely challenging.

Thermal properties of metal hydrides have dependencies on hydrogen pressure, metal hydride temperature, absorbed hydrogen concentration, metal hydride particle size, and porosity. Experiments were recently performed at the Purdue University Hydrogen Systems Laboratory (HSL) to measure the thermal properties of $Ti_{1.1}CrMn$ [22]. The hydride had particle ranging from 2 to 10 μm. Measurements were performed using the transient plane source (TPS) method, which is a variation of the hot wire technique. It directly measures thermal conductivity and diffusivity of hydride, and knowing the packing density, heat capacity is calculated. From the temperature profile within the metal hydride powder, contact resistance is also calculated. Hydrogen pressure in these property measurement experiments was increased from 2.9 to 253 bar. Thus, the properties were measured as a function of hydrogen pressure and absorbed hydrogen concentration.

These and other thermal properties are also available from the literature. Suda et al. [15] measured the thermal conductivity of $TiMn_{1.5}$ under steady state conditions. For a particle size of 400 μm, they measured k_{MH} between 0.5 and 1.2 W/m K as hydrogen pressure was increased from 0.5 to 40 bar. With increasing pressure, the added hydrogen atoms provided additional conduction pathways thereby increasing the thermal conductivity. Using the TPS method at HSL, k_{MH} of $Ti_{1.1}CrMn$ was measured to be around 1 W/m K [22] depending on packing density (thus porosity) and particle size. Thus, in most calculations in the present study, a constant k_{MH} of 1 W/m K is assumed and in a later section it is varied between 0.2 and 10 W/m K for sensitivity analysis. It was observed that specific heat increases as a function of hydrogen pressure and the hydriding reaction progress. Below 150 bar, $c_{p,MH}$ was calculated to be about 500 J/kg K. Increasing the pressure further, increased $c_{p,MH}$ to a maximum value of around 1000 J/kg K at the highest pressure of 253 bar [22]. In this study, $c_{p,MH}$ is assumed to be 500 J/kg K. Continuous expansion and contraction due to hydrogen absorption and desorption causes the hydride bed to move, resulting in poor contact with the adjoining surface. The contact resistance, R_{tc} was calculated in [22] to vary between 400 and 1800 mm² K/W as a function of hydrogen pressure and number of hydriding cycles. Dedrick et al. calculated the contact resistance for 20–44 mm sodium alanate samples [23]. Between the hydride particles and the measurement probe they calculated a value of about 3000 mm² K/W, while between the hydride particles and the container wall they calculated a high R_{tc} of 20,000 mm² K/W, possibly due to very poor contact and lack of particle packing. Due to the dependence of R_{tc} on a number of fac-

tors such as particle size, shape, porosity, nature of contact surface, and pressure, it is a very difficult parameter to control or characterize. Because the present study concerns moderately packed (rather than loose powder) hydride heat exchangers, R_{tc} is varied in the present analysis between 0 and 2000 mm² K/W; higher values are examined in a later section for sensitivity analysis. The packing density is assumed to be 2500 kg/m³, which is the density intended for future experimental work at HSL. Based on a $Ti_{1.1}CrMn$ theoretical solid bulk density of 6200 kg/m³, this packing density corresponds to 60% porosity. The reason for such high porosity is that, once activated, $Ti_{1.1}CrMn$ particles attain very sharp edges and corners with small particle size [22]. Therefore, the goal here is to achieve moderate compaction that reduces contact resistance but not very high compaction that might crush or deform the particles. Also, metal hydrides are known to expand by up to 30% during hydriding, therefore the 60% porosity allows for the hydride expansion.

Some of the kinetic parameters of the metal hydride were measured while others were obtained from the literature. The maximum hydrogen storage capacity of $Ti_{1.1}CrMn$ was measured to be 1.5 wt%. Suda et al. calculated activation energy, E_a, and activation rate, C_a, values during the hydriding of $LaNi_5$ of 20.7 kJ/mol-H_2 and 54.7 s^{-1}, respectively [24]. But for $Ti_{0.8}Zr_{0.2}Cr_{0.8}Mn_{1.2}$, they measured three to eight times faster reaction rates compared to $LaNi_5$ depending on temperature. Based on experiments conducted at HSL, C_a for $Ti_{1.1}CrMn$ was calculated at 150 s^{-1}. Suda et al. [15] studied Ti–Cr–Mn alloys and measured alloy kinetics properties by varying the relative composition of each of the three metals. They noted that even a small change (10%) in the content of any metal caused a significant change in alloy properties. For $Ti_{1.1}CrMn$, they measured standard enthalpy difference (heat of formation) and entropy difference for dissociation (dehydriding) values of −22 kJ/mol-H_2 and −113.4 kJ/mol-H_2 K, respectively. They did not specify these values for hydriding. But for metal hydrides, the heat of desorption is different from the heat of absorption. Heat of formation during hydriding is lower compared to dehydriding. Recent experiments performed with $Ti_{1.1}CrMn$ at HSL have yielded enthalpy and entropy change values of ΔH_r = 14.4 kJ/mol-H_2 and ΔS = −91.3 kJ/mol-H_2 K, respectively, during hydriding. Table 2 lists the thermal and kinetic properties of $Ti_{1.1}CrMn$ used in the present analysis.

Using these properties, geometrical parameters like metal hydride thickness, and heat transfer parameters, like coolant temperature and heat transfer coefficient, were varied in the model to study their effects on the hydriding process is pursuit of practical means for maximizing the reaction rate.

3. Effects of metal hydride powder thickness

3.1. Calculation of maximum metal hydride thickness

Hydriding is a temperature-dependent process, the rate of which is greatly influenced by how quickly heat can be removed from the metal hydride powder. Hydriding proceeds faster at locations closer to the cooling surface, where heat transfer rate is higher than at locations farther away. Additionally, it is a self-limiting reaction, i.e., the rate of reaction decreases as the reaction proceeds further. Thus, the maximum distance between the metal hydride powder and the cooling surface is the most important design parameter when hydriding needs to be completed in a short time, 5 min for the present study. Beyond a certain distance from the cooling surface, it is practically impossible to complete the hydriding process in under 5 min. In order to estimate this maximum thickness, the model equations described in the previous section were solved for different distances ranging from 5 to 50 mm under

Table 2
Metal hydride properties used in model.

Kinetic	
Enthalpy of formation	$\Delta H_r = -14390$ J/mole-H_2
Entropy of formation	$\Delta S = -91.3$ J/mole-H_2
Activation energy	$E_a = 20.7$ kJ/mole-H_2
Activation rate	$C_a = 150$ s^{-1}
H_2 storage capacity	1.5 wt%
Thermal	
Packing density	$p_{MH} = 2500$ kg/m^3
Effective thermal conductivity	$k_{MH} = 1$ W/m K
Specific heat	$c_{p,MH} = 500$ J/kg K
Contact resistance	$R_{tc} = 2000$ mm^2 K/w
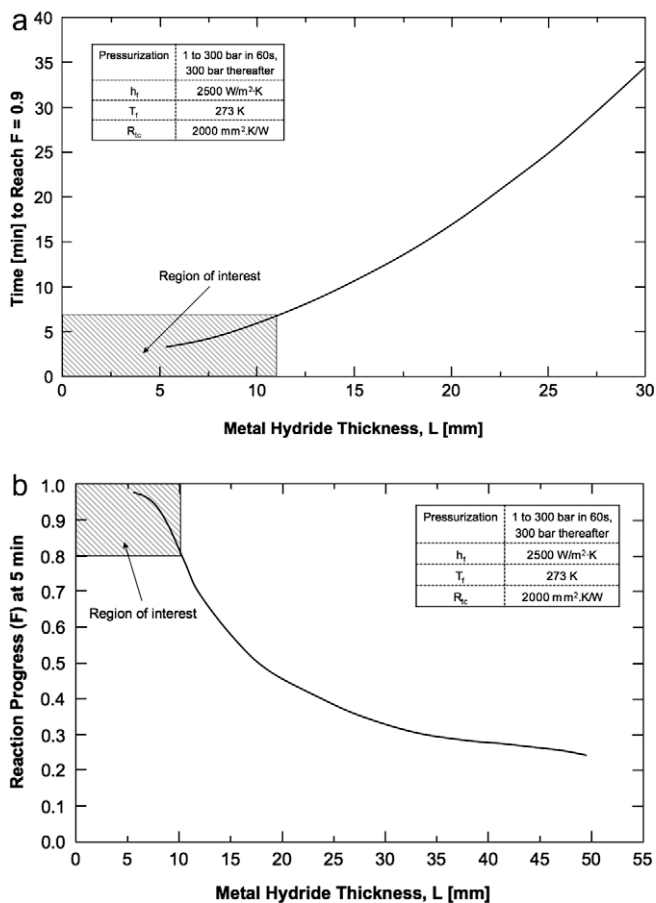
Fig. 3. (a) Variation of fill time with metal hydride thickness for 90% completion of hydriding reaction. (b) Variation of reaction progress after 5 min with metal hydride thickness.

practical operating conditions. The kinetic and thermal properties of the HPMH used in the model are listed in Table 2.

Shown in Fig. 3(a) is the variation of the time required for 90% of the hydriding reaction to be completed with metal hydride thickness. The 90% value used here is a practical measure of reaction completion because it takes a very long time between 90% and 100% completion due to the self-limiting nature of the hydriding reaction. Hence, subsequent discussions in this paper on fill time refer to the time needed to complete 90% of the complete hydriding. Fig. 3(a) shows that, under the assumed set of parameters, a fill time of 5 min requires that the metal hydride thickness be kept below 10 mm. For metal hydride thicknesses above 10 mm, the fill time increases well above the desired 5 min and reaches as high as 34 min for a 30 mm thickness. Fig. 3(b) shows the effect of metal

hydride thickness on reaction progress at the end of 5 min. For a hydride thickness of less than 10 mm, at least 80% of the metal hydride finishes hydriding. Increasing the hydride thickness decreases the fraction of reaction completion at 5 min substantially.

Fig. 3(a and b) prove that, under the assumed conditions, achieving the required fill time of 5 min requires the metal hydride thickness to be limited to 10 mm. These results are different for other metal hydrides (or other hydrogen storage materials) because of differences in both the kinetic and thermal properties. The hydride thickness can be increased to increase hydride storage capacity by improving the heat transfer parameters, such as decreasing the coolant temperature, increasing the coolant flow rate, or reducing the contact resistance. To study the effects of various parameters and means to improve the fill time, a 15 mm metal hydride thickness, which encompasses the optimum 10 mm thickness, is used.

3.2. Effects of distance from cooling surface

The behavior of the metal hydride at different distances from the cooling surface helps further the understanding of the importance of metal hydride thickness. Fig. 4(a–c) shows the variations over time of the volumetric heat generation, temperature and reaction progress at different locations within the metal hydride. Five locations separated by one fourth of the 15 mm width are considered. The location at the interface between the metal hydride and metal surface of the cooling passage is numbered 1, and the location farthest from the metal surface along the adiabatic boundary (see Fig. 2(b)) is numbered 5. The parameters used are the same as those listed in Table 2 and it is assumed that the metal hydride is initially at 20 °C before the hydrogen is charged. During the charging process, the hydrogen gas is supplied at a pressure that increases from 1 to 300 bar in 60 s; the pressure is then maintained at 300 bar until the hydriding process is complete.

Fig. 4(a) shows the volumetric rate of heat generation due to pressurization and hydriding over time at the five locations. No heat is generated due to hydriding in the first few seconds; the only source of heating during this early period is pressurization. Since the metal hydride is initially at 20 °C, the corresponding equilibrium pressure is around 100 bar. Hence, hydriding will not start until either the pressure is at least above 100 bar or the metal hydride has cooled to a lower temperature where the corresponding equilibrium pressure is lower than the metal hydride tank pressure.

The driving potential for the hydriding reaction is the difference between the metal hydride tank pressure and equilibrium pressure; the larger this difference is the faster is the reaction rate. The rate can be increased by either increasing the pressure or reducing the metal hydride temperature. During the first 60 s, pressure is assumed to increase linearly from atmospheric to 300 bar. During this pressurization ramp, the metal hydride temperature increases. If sufficient cooling is provided during a small pressure increment during the pressure ramp, the metal hydride temperature will be maintained below the equilibrium temperature and the reaction continues as the pressure increases by a second increment. However, if the cooling is insufficient, the metal hydride temperature reaches the equilibrium temperature and the reaction stalls. The reaction can then resume if either the pressure is sufficiently increased or the temperature sufficiently reduced. The present model assumes the pressure is maintained constant at the end of the 60 s period. As a result, the only way to increase the driving potential (*i.e.*, lower equilibrium pressure) is to decrease the metal hydride temperature. Thus, at each of the five locations, peak heat generation rate is observed at the end of the pressurization ramp, after which the heat generation drops significantly due to the decreased rate of hydriding.
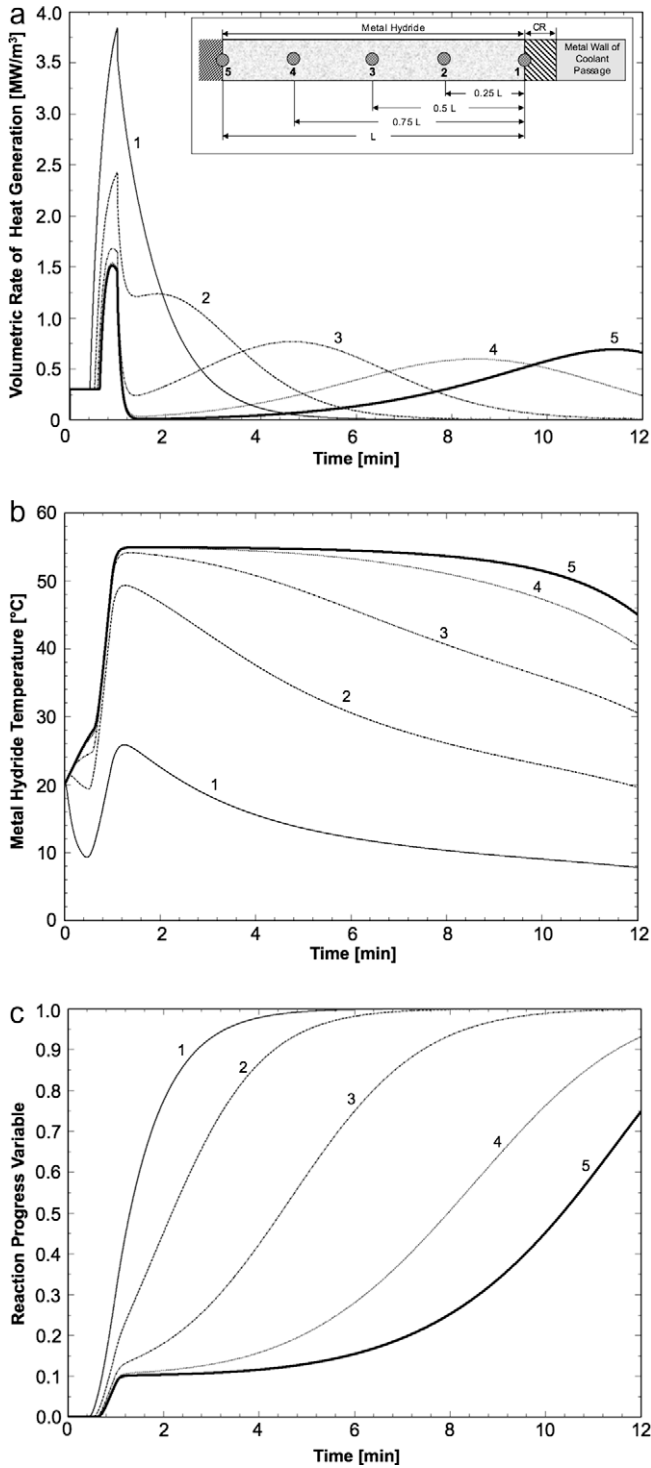
Fig. 4. Variations of (a) heat generation rate, (b) temperature, and (c) reaction progress with time at five locations within metal hydride.

Fig. 4(a) shows that location 1, which is closest to the coolant passage, is associated with very high heat transfer rates. As a result, metal hydride temperatures at this location are always lower than the equilibrium temperature and location 1 has high reaction rates. Similarly, location 2, which has a slower cooling rate than location 1, is always below the equilibrium temperature. At location 3, the heat generation rate drops significantly at the end of the pressurization ramp. The reaction rates then increase once the temperature starts decreasing as a result of cooling. At around 5 min the reac-

tion rate is highest, causing a peak in the heat generation rate. This peak in the heat generation rate can be observed shifting to the right along the time axis as we move away from the cooling surface. Being farthest away from the cooling surface, locations 4 and 5 do not receive sufficient cooling to reduce their temperatures quickly enough. At these two remote locations, the reaction stops at the end of the pressurization ramp because they reach equilibrium temperature. Location 4 starts reacting again at 2 min and reaches peak reaction rate at 8.2 min, while location 5 does not reach its peak reaction rate until after 11.5 min. At the end of 12 min, the entire metal hydride finishes more that 90% of the hydriding reaction. It should be noted that the area under the volumetric rate of heat generation curve equals the total heat released while its ratio to the enthalpy of formation at any point on the curve equals the reaction progress.

Fig. 4(b) shows the variation of metal hydride temperature with time for each of the five locations. During the first few seconds before the start of hydriding, only pressurization contributes to heat generation. At locations closer to the cooling passage, the rate of cooling is higher than the rate of heat generation due to pressurization. As a result, we see that at locations 1 and 2, the temperature decreases during the period when no hydriding is occurring. At locations 4 and 5, the cooling rate is slower and the temperature rises higher than at location 3. Thus, the farther the metal hydride is from the coolant passage, the higher is the temperature reached during the pressurization, and the longer is the time it would take to start hydriding. The equilibrium temperature corresponding to the maximum pressure of 300 bar is 55 °C. Locations 1 and 2 never reach this equilibrium temperature. While location 1 reaches a maximum temperature of only 25 °C, location 2 reaches 49 °C indicating high heat transfer rates at both of these locations. Also, the temperatures at these locations drop rapidly after the pressurization ramp. Locations 3, 4 and 5 reach the equilibrium temperature of 55 °C at the end of the pressurization ramp. But, while the temperature at location 3 starts dropping immediately after the pressurization ramp, albeit slowly, temperatures at locations 4 and 5 remain at 55 °C for 2 and 3.5 min, respectively, before any drop in temperature is observed. It is to be noted here that the temperature never increases above the equilibrium temperature. This is because, at the equilibrium temperature, the metal hydride tank pressure is same as the equilibrium pressure and there is no driving potential for hydriding, which causes the reaction and, hence, heat generation to stop. At location 3, the temperature starts dropping at a faster rate after 5 min suggesting that most of the reaction is over. However, at location 5, which is 15 mm from the coolant passage, it takes more than 6.5 min to drop by 1 °C to reach 54 °C and takes more than 10 min to drop below 50 °C. Thus, maintaining low metal hydride temperatures is the most important factor in achieving fast filling rates. As the temperature decreases, the driving potential for hydriding increases, which leads to faster filling rates.

Fig. 4(c) shows the variation of the reaction progress over time at the five metal hydride locations. As discussed earlier, no hydriding reaction is observed in the first few seconds of pressurization. Also, the reaction first starts at locations closest to the coolant passage and then proceeds to the more remote locations. Fig. 4(c) shows no decrease in the reaction rate at locations 1 and 2 after the pressurization ramp ends. These two locations are associated with very high heat transfer rates and, from the reaction profiles, it can be seen that the reaction is not heat transfer limited but kinetics limited. This means that were the heat transfer rates to be increased by increasing the coolant flow rate or decreasing the coolant temperature, the reaction progress at locations 1 and 2 would still remain the same. The time it takes to complete 100% reaction from 90% is about 2 to 3 min at each location. This is a long time considering the target fill time of 5 min. With the fill

time being the time to finish 90% of the hydriding, the effective material storage capacity is 90% of the maximum hydrogen storage capacity. At the other locations, the reaction slows down and may even stop (especially at location 5) until the metal hydride is cooled enough to bring its temperature below the equilibrium temperature, after which the reaction continues until the hydriding is complete. Thus, the time it takes to completely the hydriding depends directly on the heat transfer rate, which, in turn, depends on the thickness of the hydride layer.

4. Parameters influencing fill rate

4.1. Non-dimensional conductance

For a given metal hydride composition, the reaction rate depends only on heat transfer parameters. Just like in any heat exchanger, heat transfer rate can be improved by increasing the conductance of the path of heat flow. In a heat exchanger, there are a number of parameters that affect heat transfer rate. And in the present application, where a reacting medium is cooled by a coolant flowing through coolant passages, heat transfer rate is affected by coolant temperature, coolant flow rate, contact resistance, thickness of metal hydride layer, and the effective conductivity of the metal hydride powder. To consolidate the influences of these parameters on the heat transfer performance and to study their relative importance to the fill rate, a new non-dimensional conductance (NDC) parameter is developed. The NDC is defined as the ratio of the maximum heat rate that can be removed from the metal hydride under a prescribed set of experimental conditions to the heat rate that would be generated for a specified thickness of metal hydride to hydride completely in the desired time.

$$\text{NDC} = \frac{\left(\frac{T_{MH,max}-T_f}{\frac{1}{h_f}+R_{tc}+\frac{L}{k_{MH}}}\right)}{\left(\frac{\Delta H_r \; (wt\%) \rho_{MH}}{MW_{H_2}} \cdot \frac{L}{t_{des}}\right)}. \tag{5}$$

The NDC is a measure of the fraction of heat generation rate due to hydriding that can be removed by the heat exchanger. A higher NDC amounts to higher heat transfer rates. $T_{MH,max}$ in Eq. (5) is the equilibrium temperature of the metal hydride corresponding to the maximum hydrogen pressure at the end of the pressure ramp. Increasing hydriding pressure increases reaction rate as well as the metal hydride equilibrium temperature. Thus, $T_{MH,max}$ is an indirect measure of pressure and a higher $T_{MH,max}$ value indicates faster hydriding rates. Eq. (5) shows a higher NDC can also be achieved by lowering the coolant temperature, T_f, or by increasing the conductance of the heat transfer path. The effect of the coolant's flow rate is implicit in the magnitude of the convective heat transfer coefficient. Another important parameter impeding heat flow is the contact resistance between the metal hydride powder and walls of the coolant passages. Contact resistance depends on powder properties, mainly size and packing density, and wall properties such as material type, surface roughness, and geometry. For a given wall material and geometry, the higher the packing density, the higher is the pressure against the wall and the lower is the contact resistance. However, there is limit to which metal hydride powder can be packed. As discussed earlier, metal hydrides are known to expand by as much as 30% during hydriding. Hence, the packing density must be such that it is just sufficient to accommodate the expansion during hydriding so that the contact resistance can be minimized. Finally, as discussed in the previous section, heat transfer rate is smaller in thicker hydride layers. Thicker layers increase the conduction resistance to the heat flow from the metal hydride particles to the coolant. Hence, the NDC decreases with increasing hydride layer thickness. On the other hand, higher metal hydride conductivity improves heat transfer rates and
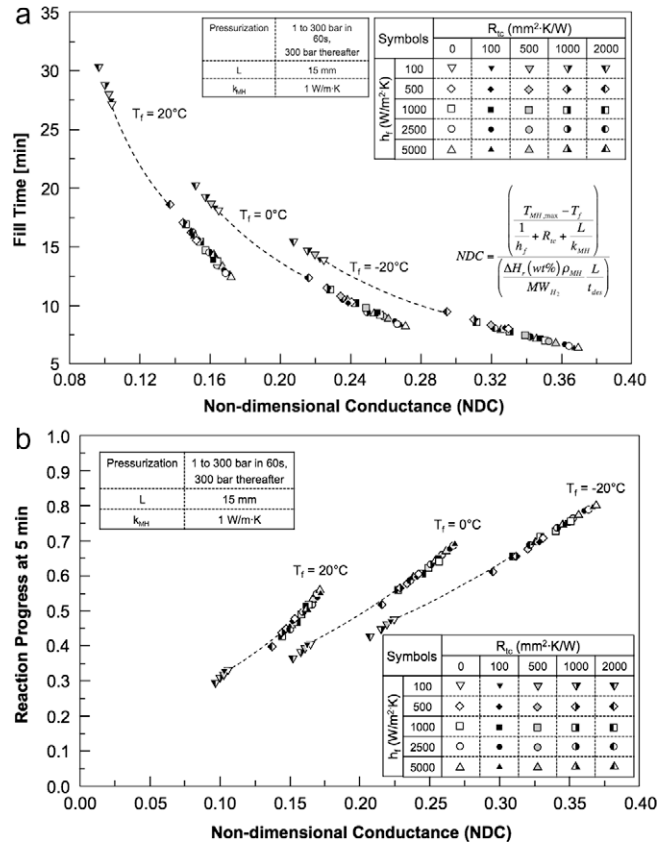
Fig. 5. Variations of (a) fill time and (b) reaction progress at 5 min for 15-mm metal hydride layer with non-dimensional conductance (NDC).

increases the NDC. The denominator in Eq. (5) is the average heat generation rate if all the metal hydride in a layer of thickness L were to be hydrided within a desired fill time t_{des}. The desired fill time t_{des} is set equal to 5 min in the present analysis.

Shown in Fig. 5(a and b) are the variations of fill time and reaction progress at the end of 5 min with NDC. These plots cover broad ranges of coolant temperatures, convective coefficients (which depend on coolant flow rate) and contact resistances. The metal hydride thickness is fixed at 15 mm and metal hydride kinetic properties are those listed in Table 2. Fig. 5(a) shows fill time decreases with increasing NDC. For a given coolant temperature, the fill time decreases monotonically with an increase in the convective coefficient or a decrease in the contact resistance. Increasing the convective coefficient from 100 to 500 W/m² K significantly reduces the fill time by as much as 50% in some cases. While increasing the convective coefficient above 500 W/m² K also reduces the fill time, the effect is far less pronounced. Increasing the convective coefficient from 2500 to 5000 W/m² K does not lead to any significant improvements (less than 5%) in fill time. Hence, while increasing the flow rates does reduce the fill time, there is a limit beyond which increasing the flow rate has very little effect on fill time. Lower contact resistances also lead to shorter fill times. However, less than 7% difference in fill time is observed when the contact resistance is increased from zero to 500 mm² K/W. Increasing the contact resistance above 500 mm² K/W causes a noticeable increase in the fill time. Comparing the slopes of the plots at different coolant temperatures, it can be seen that the contact resistance and convection coefficients have stronger effects at higher coolant temperatures than at lower temperatures. Also, reducing the coolant temperature is the most practical and effective way to reduce the fill time. Under a given set of conditions,
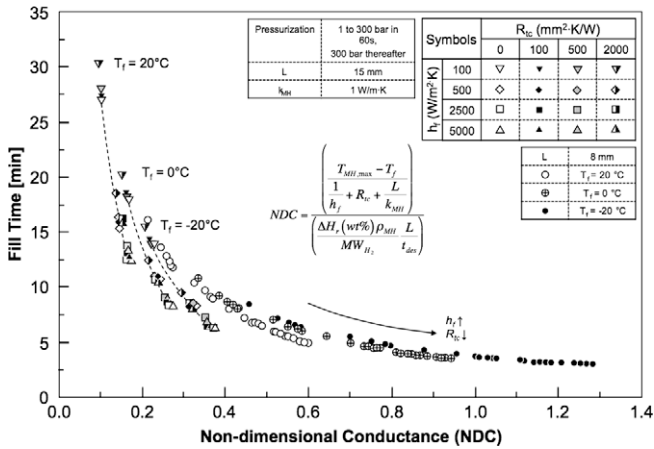
Fig. 6. Variation of fill time with non-dimensional conductance for 8 mm and 15 mm metal hydride layers.

Fig. 7. Effect of metal hydride thermal conductivity on H_2 fill time.

Fig. 8. Effect of coolant temperature on H_2 fill time.

reducing the coolant temperature from 20 °C to 0 °C can, in some cases, reduce the fill time by as much as 10 min.

Fig. 5(b) shows the reaction progress at the end of 5 min plotted against the NDC for a 15-mm metal hydride layer. These results show that, within the range of experimental conditions varied in this analysis, a fill time of 5 min is not achievable since all reaction progress values fall below 90%. This means that for this particular metal hydride powder, it is practically impossible to achieve a fill time of 5 min if the layer thickness is 15 mm or greater without improving the effective thermal conductivity or reducing the packing density.

It should be noted that, for a given NDC value, different fill times are possible depending on the relative importance of different parameters. In other words, there is more than one way to achieve a particular NDC value that would not necessarily yield the same fill time.

Fig. 6 compares the variation of fill time with NDC for an 8-mm metal hydride layer to that of the 15-mm layer shown in Fig. 5(a). Under a given set of conditions, reducing the thickness from 15 to 8 mm significantly reduces the fill time while increasing the NDC. Fig. 6 shows that there is a consistent relationship between the reaction rate and the NDC. The NDC can therefore be used as a characteristic parameter to estimate and study the effects of various parameters on reaction rate. Increasing the NDC beyond 0.8 does not cause much increase in the filling rate because the kinetic limit is reached.

4.2. Effects of thermal conductivity of HPMH

Shown in Fig. 7 is a plot of the fill time as a function of the effective thermal conductivity of the metal hydride powder. At low thermal conductivity, the fill times are very long, approaching 40 min for an effective thermal conductivity of 0.2 W/m K compared to 10 min for 1 W/m K. Thermal conductivity has a weak effect above 2 W/m K. For example, increasing the conductivity from 5 to 10 W/m K decreases the fill time from 5.1 to only 4.5 min. As discussed earlier, high-pressure metal hydrides generally have low intrinsic thermal conductivity. The process of hydriding does not have any noticeable effect on thermal conductivity, however it does increase with an increase in the hydrogen pressure. The effective conductivity of metal hydride powders can be improved with additives such as aluminum powder or carbon nanotubes. While additives increase the effective conductivity, they also reduce the amount of metal hydride in the heat exchanger. Thus, the use of additives to improve the thermal conductivity is a tradeoff
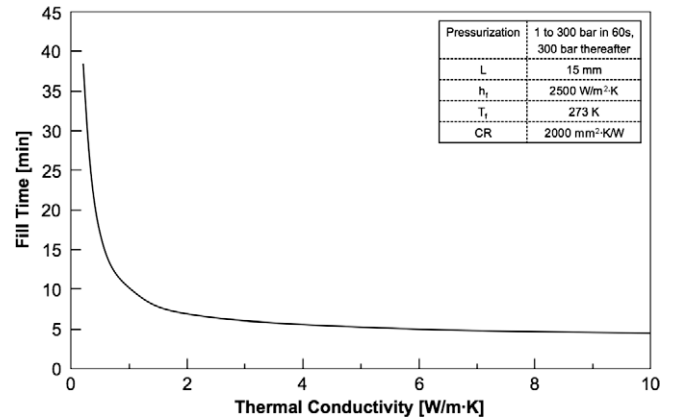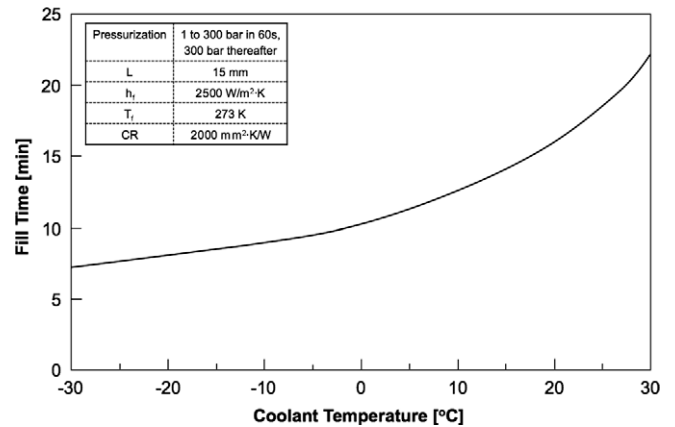
between reducing the fill time and compromising the hydrogen storage capacity.

4.3. Effects of coolant temperature

Fig. 8 shows the fill time decreases monotonically with decreasing coolant temperature. Also, the influence of coolant temperature is more pronounced at higher temperatures. Decreasing the coolant temperature reduces the fill time until the kinetic limit is reached, after which it has no effect on fill time. Decreasing the coolant temperature has a direct and significant influence in increasing both the heat transfer rate and the reaction rate. This is especially important in a hydrogen storage system in which thermal parameters like contact resistance change as a function of the hydrided state of the metal hydride. Being externally controlled, coolant temperature can be the most effective design parameter to achieve a desired fill time.

5. Sensitivity Analysis

Fig. 9 shows the relative influence of key parameters and metal hydride properties on fill time. The fill time is calculated for each parameter by independently varying its magnitude within a practical range, while all other parameters are held constant at nominal values. Under the listed set of nominal values, it takes 10.6 min to complete 90% of the hydriding reaction for a 15-mm layer of metal hydride.

Fig. 9 shows that the fill time is most sensitive to the effective thermal conductivity of the metal hydride and the coolant
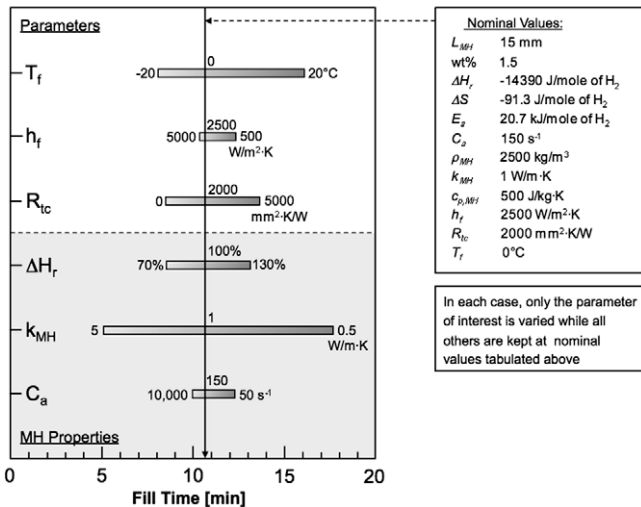
Fig. 9. Sensitivity analysis of various parameters and properties influencing fill time.

temperature. The sensitivity to the thermal conductivity assumes greater significance because it changes during the process of hydriding and also depends on such parameters as hydride particle size, shape, and packing density. The value of k_{MH} is varied between 0.5 and 5 W/m K. The lower range from 0.5 to 1 W/m K corresponds to values measured for pure metal hydride powder [16,22]. Increasing k_{MH} from 0.5 to 1 W/m K decreases the fill time considerably, from 17.7 to 10.7 min. Increasing k_{MH} from 1 to 5 W/m K further reduces the fill time to 5 min, albeit at a lesser rate than between 0.1 and 1 W/m K. Thus, fill time is more sensitive to k_{MH} at lower k_{MH} values and a minimum value of about 1 W/m K is necessary for practical fill times. Thermal conductivity can be improved by mixing metal hydride powder with additives such as aluminum powder and carbon nanotubes. While it is advantageous to improve the thermal conductivity, doing so with additives should be weighed against a corresponding reduction in storage capacity.

Fig. 9 shows that lowering the coolant temperature by 20 °C reduces the fill time by 2.6 min, however, an increase in coolant temperature by 20 °C increases fill time by 5.3 min. Thus, fill time is more sensitive to coolant temperature at higher values. Lowering the coolant temperature is an effective means to reducing fill time, especially since it is an externally controlled parameter. The selection of an appropriate coolant temperature is the result of a trade-off between desired fill time and cost of the cooling system.

Contact resistance is the third parameter that appears to have an appreciable influence on fill time. This parameter depends on a variety of factors and is difficult to either control or characterize. For metal hydride particles, the contact resistance is calculated to vary between 400 and 3000 mm² K/W [23]. As the hydride powder expands and contracts due to hydriding cycles, R_{tc} may further increase due to movement of the hydride powder bed. Fig. 9 shows fill time is sensitive to R_{tc} and it is important to maintain low R_{tc} values to achieve short fill times.

Coolant flow rate has a limited effect on fill time. Increasing the convective coefficient from 2500 to 5000 W/m² K reduces the fill time by less than a minute. Reducing h_f to 500 W/m² K also has a small effect and increases the fill time to 12.2 min. However, reducing h_f to 100 W/m² K increases fill time to 20 min. Thus, it is important to maintain a coolant flow rate above a minimum limit, but above this limit the effect of flow rate is insignificant.

The kinetic properties of the metal hydride greatly depend on their exact composition. Changing the relative composition of Ti–Cr–Mn by just 10% can change the enthalpy of reaction by as much as 18% [15]. To study the effect of change in the enthalpy of reac-

tion on fill time, ΔH_r was varied between 70% and 130% of the nominal value. Along with the enthalpy of reaction, the entropy change is also modified such that equilibrium pressure corresponding to the peak temperature is the same in each case. Fig. 9 shows higher values of enthalpy of reaction, which amount to higher rates of heat generation, prolong fill time. Hence, it is important to suitably modify the heat exchanger design for each metal hydride so that the desired fill time is reached.

Activation rate, C_a, is a measure of the reaction rate of the metal hydride. For LaNi5, $C_a = 54.7$ s^{-1} while for Ti$_{0.8}$Zr$_{0.2}$Cr$_{0.8}$Mn$_{1.2}$, $C_a = 500$ s^{-1} [16]. Fig. 9 shows fill time is quite insensitive to C_a, with $C_a = 50$ s^{-1} yielding a fill time of 12 min compared to 10 min for $C_a = 10,000$ s^{-1}.

Overall, Fig. 9 shows that the most practical and effective means to reducing fill time are to (1) enhance the thermal conductivity of the metal hydride, (2) reduce the coolant's temperature, and (3) reduce the thermal contact resistance.

6. Conclusions

In order to achieve industry targets for on-board hydrogen storage, it is important to improve current material properties as well as develop new materials with high storage capacities. It is also important to simultaneously design and optimize the storage systems. Work presented here forms a basis for practical heat exchanger design used in storage systems employing materials with high rates of heat generation during refueling. Key conclusions from this study are as follow.

1. The heat exchanger is the most important component of a hydrogen storage system utilizing high-pressure metal hydrides. It has to perform the task of storing the metal hydride while providing sufficient cooling to achieve the required short fill time.
2. Metal hydride layer thickness (maximum distance between the metal hydride powder and the cooling surface) is the most important design parameter for the heat exchanger. For Ti$_{1.1}$CrMn, this thickness must be kept below 10 mm to achieve a fill time of 5 min.
3. Metal hydride particles closest to the cooling surface react at a faster rate compared to those located farther away. With a sufficient cooling rate, the hydride quickly cools to below the equilibrium temperature. However, if the cooling rate is insufficient, the hydride remains at equilibrium temperature for an extended period and the reaction stops.
4. A new parameter called non-dimensional conductance (NDC) is developed. It is a measure of the fraction of heat generation rate due to hydriding that can be removed by the heat exchanger. NDC can be used as a characteristic parameter to estimate the effects of various parameters on the reaction rate.
5. Fill time is sensitive mostly to the effective thermal conductivity of the metal hydride and the coolant's temperature, followed by the contact resistance. While it is important to maintain the coolant's flow rate above a minimum limit, there are no additional benefits to increasing the flow rate above this limit.
6. Contact resistance is unavoidable when using powders for hydrogen storage, and is also the most difficult parameter to control or characterize. Contact resistance may be minimized by moderate packing of the powder within the heat exchanger to completely accommodate the powder in its fully hydrided (expanded) state, but without crushing the sharp-edged fine particles.

References

[1] L. Schlapbach, A. Züttel, Hydrogen-storage materials for mobile applications, Nature 414 (2001) 353–358.

[2] DOE, Hydrogen, fuel cells and infrastructure technologies program, multi-year research, development and demonstration plan: planned program activities for 2005–2015, Energy Efficiency and Renewable Energy, U.S. Department of Energy, Washington, DC, 2007.

[3] J. Zhang, T.S. Fisher, P.V. Ramachandran, J.P. Gore, I. Mudawar, A review of heat transfer issues in hydrogen storage technologies, J. Heat Transfer 127 (2005) 1391–1399.

[4] G. Walker, Solid-State Hydrogen Storage: Materials and Chemistry, Woodhead publishing, Cambridge, England, 2008.

[5] N. Takeichi, H. Senoh, T. Yokota, H. Tsuruta, K. Hamada, H. Takeshita, H. Tanaka, T. Kiyobayashi, T. Takano, N. Kuriyama, Hybrid hydrogen storage vessel a novel high pressure hydrogen storage vessel, combined with hydrogen storage material, Int. J. Hydrogen Energy 28 (2003) 1121–1129.

[6] G.D. Berry, S.M. Aceves, Onboard storage alternatives for hydrogen vehicles, Energy Fuels 12 (1998) 49–55.

[7] S.M. Aceves, G.D. Berry, J. Martinez-Frias, F. Espinosa-Loza, Vehicular storage of hydrogen in insulated pressure vessels, Int. J. Hydrogen Energy 31 (2006) 2274–2283.

[8] A. Zuttel, Materials for hydrogen storage, Mater. Today 6 (2003) 24–33.

[9] D. Mori, K. Hirose, Recent challenges of hydrogen storage technologies for fuel cell vehicles, Int. J. Hydrogen Energy 34 (2009) 4569–4575.

[10] E. Poirier, A. Dailly, Thermodynamic study of the adsorbed hydrogen phase in Cu-based metal-organic frameworks at cryogenic temperatures, J. Phys. Chem. C 112 (2008) 13047–13052.

[11] G. Thomas, S. Satyapal, A brief overview of hydrogen storage issues and needs, DOE FreedomCAR Joint Tech Team Meeting: Delivery, Storage and Fuels Pathways Tech Teams, Columbia, MD, 2007.

[12] S. Mellouli, F. Askri, H. Dhaou, A. Jemni, S. Ben Nasrallah, A novel design of a heat exchanger for a metal-hydrogen reactor, Int. J. Hydrogen Energy 32 (2007) 3501–3507.

[13] S. Mellouli, F. Askri, H. Dhaou, A. Jemni, S. Ben Nasrallah, Numerical study of heat exchanger effects on charge/discharge times of metal-hydrogen storage vessel, Int. J. Hydrogen Energy 34 (2009) 3005–3017.

[14] Y. Kojima, Y. Kawai, S. Towata, T. Matsunaga, T. Shinozawa, M. Kimbara, Development of metal hydride with high dissociation pressure, J. Alloys Compd. 419 (2006) 256–261.

[15] S. Suda, Y. Komazaki, N. Kobayashi, Effective thermal conductivity of metal hydride beds, J. Less-Common Met. 89 (1983) 317–324.

[16] M. Botzung, S. Chaudourne, O. Gillia, C. Perret, M. Latroche, A. Percheron-Guegan, P. Marty, Simulation and experimental validation of a hydrogen storage tank with metal hydrides, Int. J. Hydrogen Energy 33 (2008) 98–104.

[17] B.D. MacDonald, A.M. Rowe, Impacts of external heat transfer enhancements on metal hydride storage tanks, Int. J. Hydrogen Energy 31 (2006) 1721–1731.

[18] A.K. Phate, M.P. Maiya, S.S. Murthy, Simulation of transient heat and mass transfer during hydrogen sorption in cylindrical metal hydride beds, Int. J. Hydrogen Energy 32 (2007) 1969–1981.

[19] F. Laurencelle, J. Goyette, Simulation of heat transfer in a metal hydride reactor with aluminum foam, Int. J. Hydrogen Energy 32 (2007) 2957–2964.

[20] U. Mayer, M. Groll, W. Supper, Heat and mass transfer in metal hydride reaction beds: experimental and theoretical results, J. Less-Common Met. 131 (1987) 235–244.

[21] A. Jemni, S. Ben Nasrallah, Study of two-dimensional heat and mass transfer during absorption in a metal-hydrogen reactor, Int. J. Hydrogen Energy 20 (1993) 43–52.

[22] S. Flueckiger, Thermal property measurements of high pressure metal hydrides, MS thesis, Purdue University, West Lafayette, IN, 2009.

[23] D. Dedrick, M. Kanouff, B. Replogle, K Gross, Thermal properties characterization of sodium alanates, J. Alloys Compd. 389 (2005) 299–305.

[24] S. Suda, N. Kobayashi, K. Yoshida, Reaction kinetics of metal hydrides and their mixtures, J. Less Common Met. 73 (1980) 119–126.